

**Neuron, Volume 105**

**Supplemental Information**

**Assemblies of Perisomatic GABAergic Neurons  
in the Developing Barrel Cortex**

**Laura Modol, Yannick Bollmann, Thomas Tressard, Agnès Baude, Alicia Che, Zhe Ran S. Duan, Rachel Babij, Natalia V. De Marco García, and Rosa Cossart**

# Figure S1. Related to Figure 1

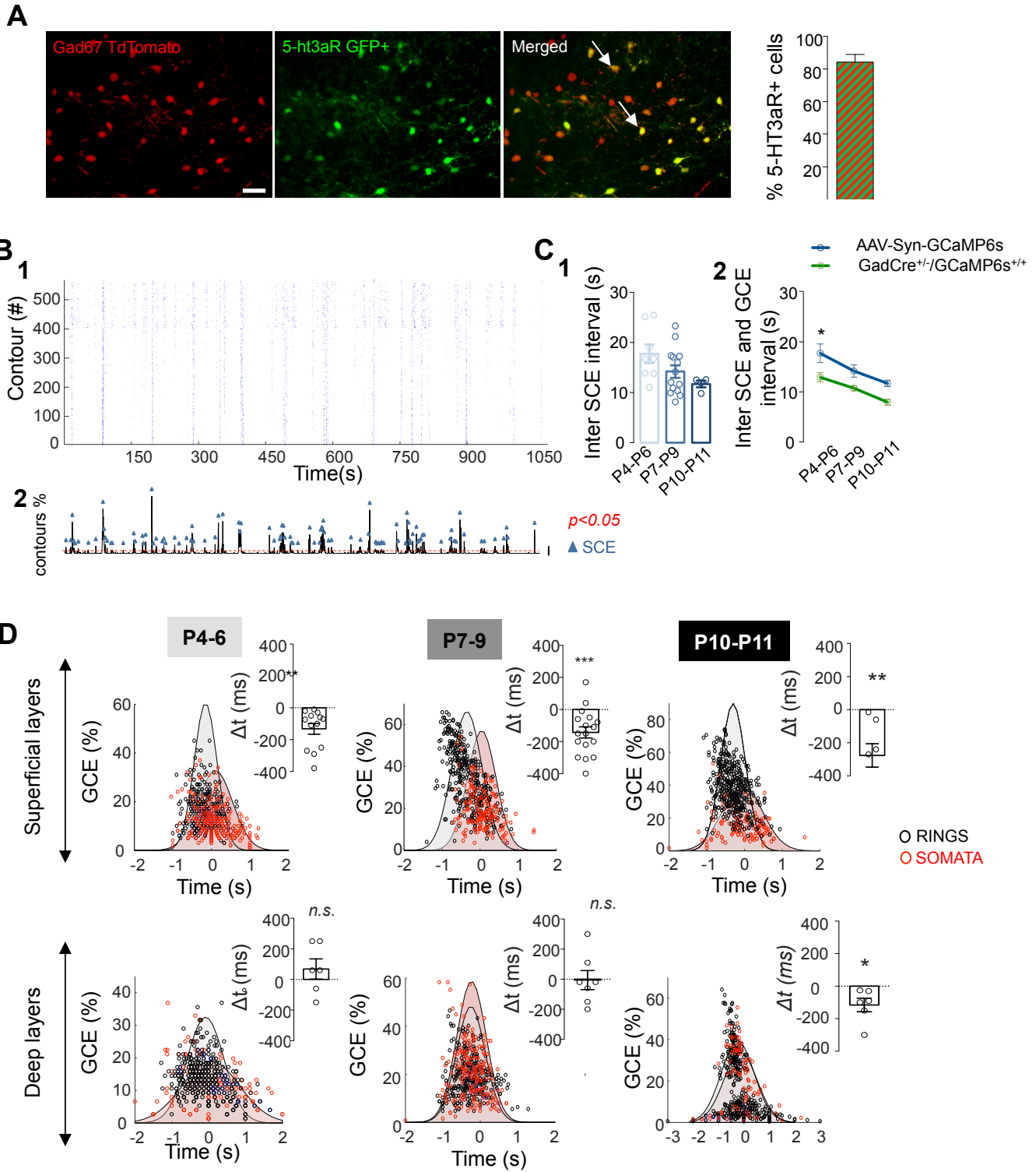


**Figure S1:** (A) Confocal images showing that the GAD67 promoter used in this study induces the expression of the reporter gene (here tdTomato using the Ai14 line, (left) in most CGE derived neurons (identified by GFP expression in the 5Ht3a-GFP mouse line, middle). This is clearly visible in the merged image (yellow, see arrows) and quantified in the bar plot showing the ratio of GFP positive cells co-expressing td-Tomato at P7 ( $84\pm 5\%$  co-labeling,  $n=12$  slices, 5 mice). Scale bar,  $50\ \mu\text{m}$ . (B) Representative rasterplot indicating the calcium events onsets occurring in a FOV where all cells are labeled using viral expression of GCaMP6s (AAV-Syn-GCaMP6s); the sum of active contours over time for that rasterplot is indicated by the histogram below (2). Blue triangles indicate Spontaneous Calcium Events (SCE) based on a statistical threshold (red dotted line,  $p<0.05$ ). (C) 1, No significant change in SCE occurrence was observed as a function of age, as shown in the box plots indicating the average time interval between SCEs in the three developmental age groups. One way ANOVA:  $F_{(2,23)}=2.69$ ,  $p=0.08$ ; 2, The comparison of SCE (blue) and GCE (green) inter event intervals indicated that GCEs occurred almost twice as often as SCEs at P4-6: two-way ANOVA: no interaction effect:  $F_{(2,75)}=0.18$ ,  $p=0.18$ . Effect on the population factor:  $F_{(1,75)}=18.09$ ,  $p<0.0001$ . Subsequent *post hoc* (Tukey's), indicates differences at P4-6,  $p<0.05$ . Values in the plots indicate mean  $\pm$  SEM. (D) Temporal organization of GCEs across cortical layers and as a function of age. Representative scatter plots of mean activation onsets and mean participation rate of SOMATA (red) and RINGS (black) in GCEs at P4-6, P7 and P10-11 in superficial and deep cortical layers. Shadowed distribution represents the underlying probability density function of RINGS (light grey) and SOMATA (light red), scaled to maximum participation rate. One-sample *t*-test of pooled difference in the mean onset ( $\Delta t$ ) between RINGS and SOMATA for all cases in each condition shows that RINGS onsets occurred significantly before SOMATA in superficial layers at P4-6 ( $t_{12}=3.90$ ,  $p=0.002$ ) and P7-9 ( $t_{16}=4.12$ ,  $p=0.0008$ ). At P10-11, RINGS were significantly activated before SOMATA in both superficial and deep layers (superficial;  $t_{(6)}=3.92$ ,  $p=0.008$  and deep:  $t_{(5)}=2.79$ ,  $p=0.038$ ). No differences between the onsets of RINGS and SOMATA could be observed in deep layers at P4-6 ( $t_5=1.037$ ,  $p=0.347$ ) or P7-9 ( $t_6=0.090$ ,  $p=0.930$ ). Distribution compared against hypothetical value 0. Each circle represents one FOV. Data in the plots are Mean  $\pm$  SEM.

# Figure S2. Related to Figure 2

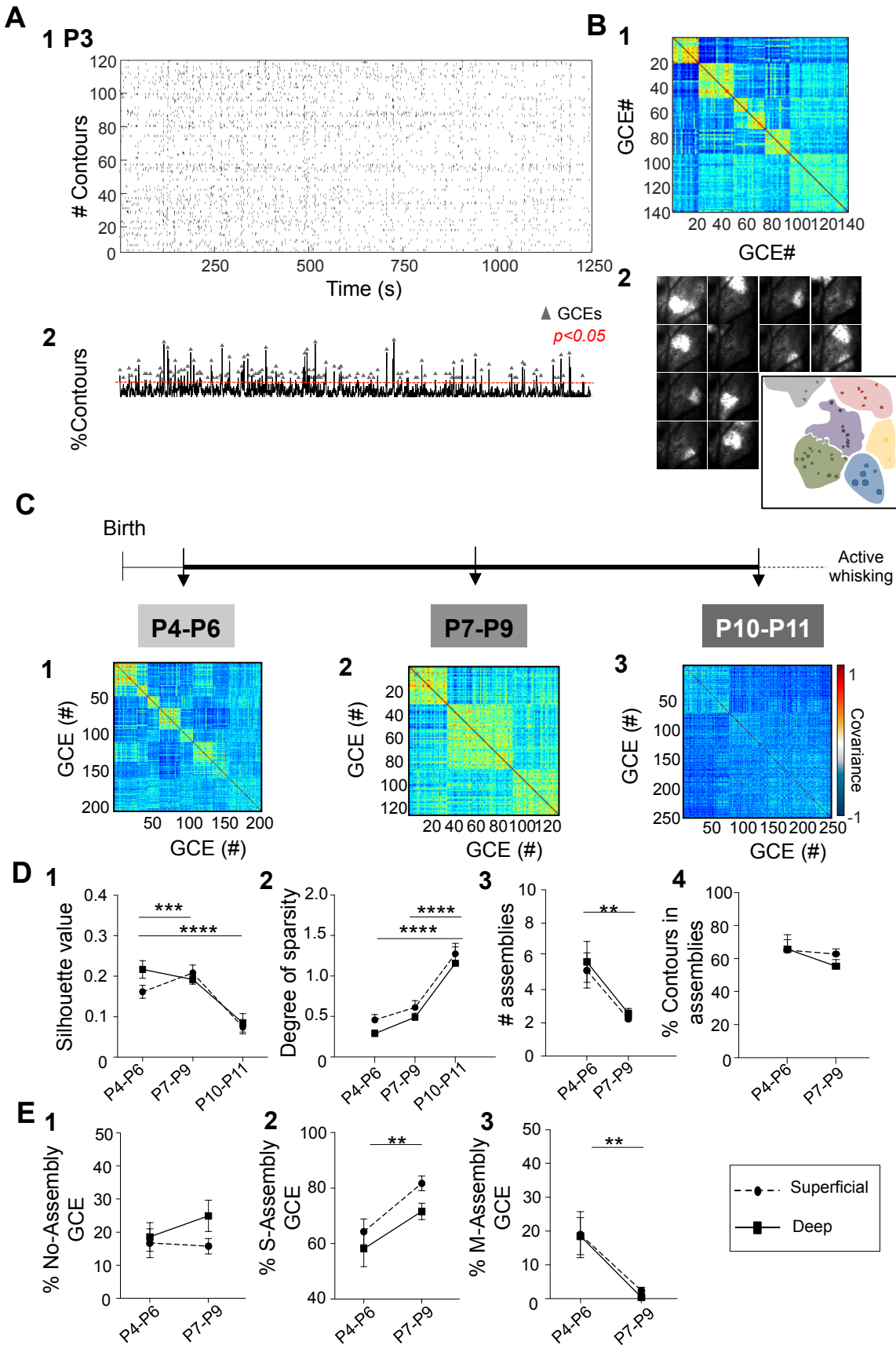
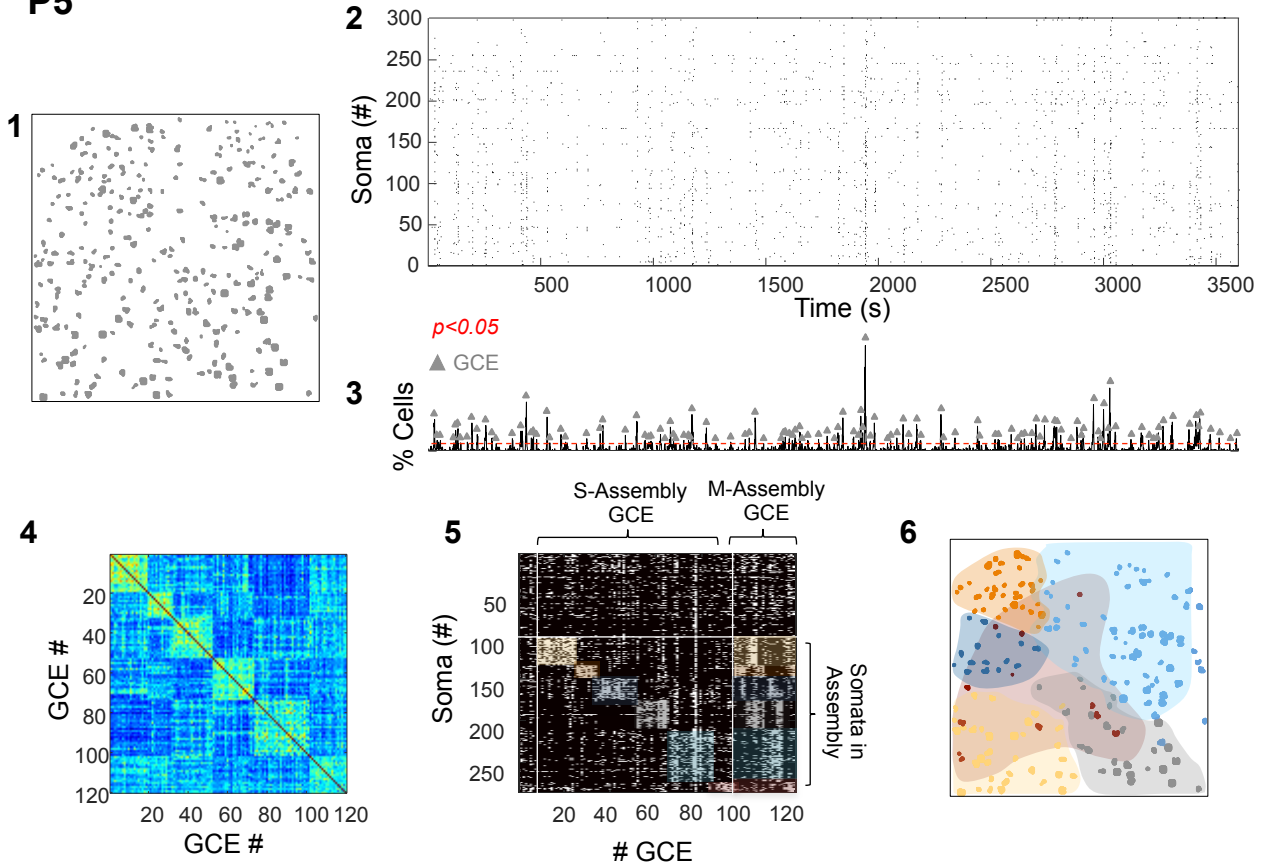


**Figure S2:** (A, B) Imaging from non-anesthetized GAD67-GCaMP6 pups at postnatal day 3 (P3). (A) **1**, Representative rasterplot indicating detected calcium events in all imaged contours as a function of time. **2**, Histogram indicating the fraction of active contours over time for the rasterplot in (1). Grey triangles indicate GABAergic calcium events (GCE) based on a statistical threshold (dotted red line,  $p < 0.05$ ). (B) **1**, Representative correlation matrix for GCEs occurring within one imaging session at P3. **2**, Movie frames showing ROIs imaged at P3 and contour map color-coded according to assembly membership. (C, D, E) Parallel development of GABAergic functional networks across layers. (C) Experiments were performed in non-anaesthetized GAD67-GCaMP6 pups between P4 and P11 as indicated in the timeline. **1**, Representative correlation matrices between all GCEs in an imaging session. (D and E) *Two-way ANOVA* analysis of changes in GCEs properties across development (*Age* factor) in superficial (dotted line) and deep layers (filled line). No significant interaction was observed between the two factors in any of the comparisons performed indicating that GABAergic dynamics in superficial and deep layers developed in parallel. Plotted significance corresponds to *Tukey's post-hoc* test or unpaired *t-test*, performed when *two-way ANOVA* analysis revealed a main simple effect. (D) **1**, Functional coherence of clustered assemblies (*Silhouette* value) decreases at P10-11 in both superficial and deep cortical layers. *Two-way ANOVA* showed no *Interaction* effect ( $F_{(2,49)}=1.29, p=0.28$ ) or *Depth* effect ( $F_{(1,49)}=0.80, p=0.37$ ) but main simple effect in the *Age* factor ( $F_{(2,49)}=17.57, p < 0.0001$ ). *Post-hoc (Tukey's)* P10-11 vs. P4-6,  $p < 0.001$  and P10-11 vs. P7-9,  $p < 0.0001$ . **2**, Network sparsity indicates the ratio of spikes occurring outside and within GCEs; this value increased at P10-11. *Two-way ANOVA* showed no *Interaction* effect ( $F_{(2,49)}=0.03, p=0.96$ ) or *Depth* effect ( $F_{(1,49)}=2.42, p=0.12$ , but simple main effect in the *Age* factor ( $F_{(2,49)}=34.29, p < 0.0001$ ). *Post-hoc (Tukey's)*: P10-11 vs. P4-6 and P7-9,  $p < 0.0001$ . **3**, Number of functional assemblies detected per imaging session decreases with age. *Two-way ANOVA* shows no *Interaction* effect ( $F_{(1,39)}=0.01, p=0.91$ ) or *Depth* effect ( $F_{(1,39)}=0.27, p=0.59$ ), but simple main effect in the *Age* factor, ( $F_{(1,38)}=14.04, p=0.0006$ ). Unpaired *t-test*,  $t_{(41)}=4.12, p=0.002$ . **4**, Fraction of active contours recruited in assemblies. *Two-way ANOVA* no *Interaction* effect ( $F_{(1,39)}=0.46, p=0.49$ ) or simple main effect (*Depth* factor:  $F_{(1,39)}=0.33, p=0.56$  or *Age* factor:  $F_{(1,39)}=1.19, p=0.28$ ). (E) **1**, Fraction of GCEs that did not display any assembly structure. *Two-way ANOVA* shows no *Interaction* effect ( $F_{(1,39)}=0.77, p=0.38$ ) or simple main effect (*Depth* factor:  $F_{(1,39)}=1.8, p=0.18$  or *Age* factor:  $F_{(1,39)}=0.43, p=0.51$ ). **2**, Fraction of GCEs that recruited a single assembly (S-Assembly). *Two-way ANOVA* no *Interaction* effect ( $F_{(1,39)}=0.20, p=0.65$ ) or *Depth* effect ( $F_{(1,39)}=3.32, p=0.07$ ), but simple main effect *Age* factor ( $F_{(1,39)}=12, p=0.001$ ). Unpaired *t-test*,  $t_{(41)}=3.92, p=0.003$ . **3**, Fraction of GCEs that recruited multiple assemblies (M-Assembly). *Two-way ANOVA* shows no *Interaction* effect ( $F_{(1,39)}=0.02, p=0.875$ ) or *Depth* effect ( $F_{(1,39)}=0.06, p=0.80$ ), but main simple effect in the *Age* factor ( $F_{(1,39)}=12.6, p=0.001$ ). Unpaired *t-test*,  $t_{(41)}=3.62, p=0.0008$ . Values are given by mean  $\pm$  SEM.

# Figure S3. Related to Figure 2

**A** P5



**B**

**P8**

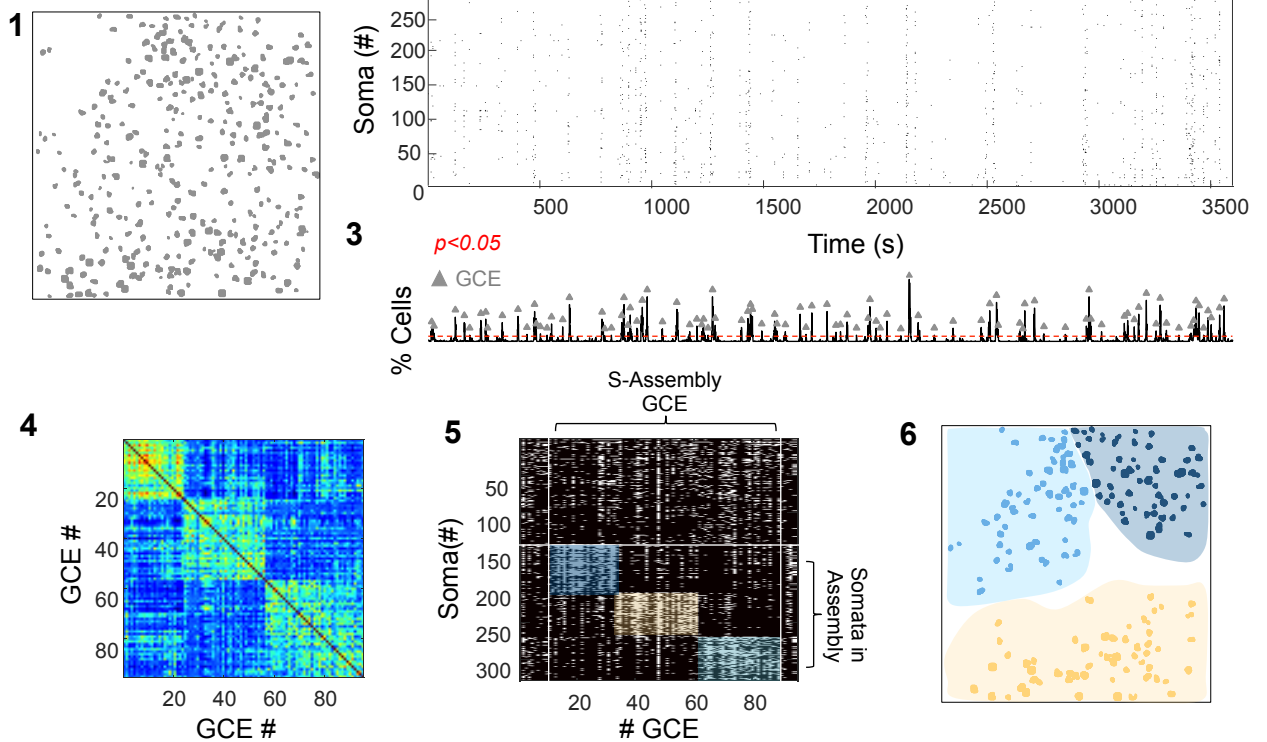


**Figure S3:** (A, B) **1**, Representative contour map of all active SOMATA within an imaging session at P5 (A) and P8 (B) corresponding to the same FOVs shown in Figure 2. **2**, Representative rasterplot indicating detected calcium events in all imaged SOMATA as a function of time. **3**, Histogram indicating the fraction of active SOMATA over time for the rasterplot in (1). Grey triangles indicate GABAergic calcium events (GCE) based on a statistical threshold (dotted red line,  $p < 0.05$ ). **4**, Correlation matrix between all GCEs the given imaging session. **5**, Representative rasterplots of GCEs recruiting specific cell bodies in assemblies. **6**, Representative movie frames showing ROIs imaged at P5 (A) and P8 (B) and contour map color-coded according to assembly membership. Scale bar, 100  $\mu\text{m}$ .

**Figure S4. Related to Figure 2 and 5**

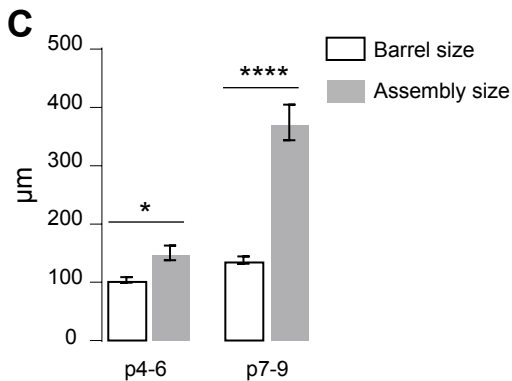
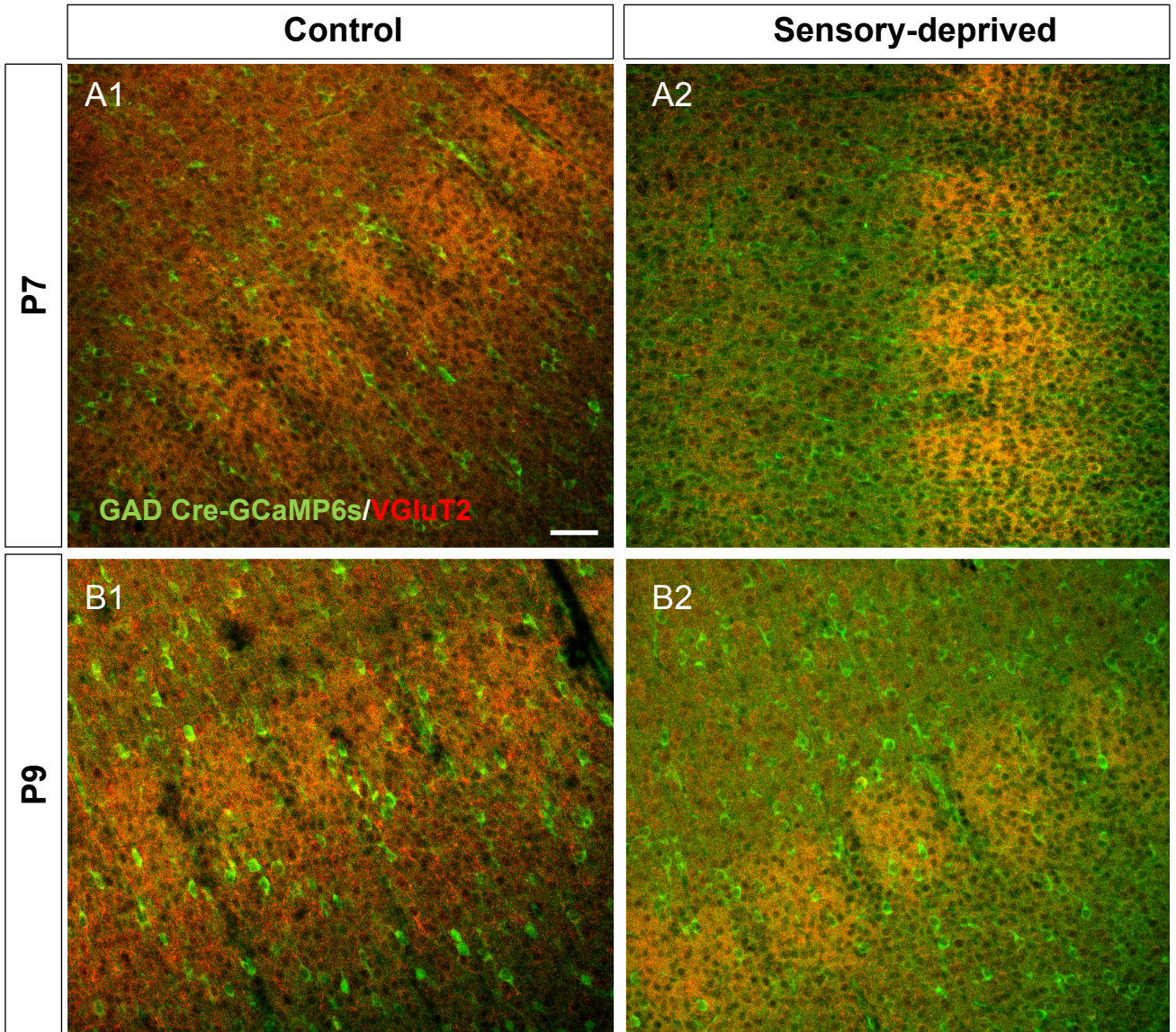


**Figure S4:** Representative confocal views showing vGlut2-immunoreactivity (red) in fixed slices from GAD67-GCaMP6 (green) mice at 7 and 9 postnatal days (**A** and **B**, respectively); the typical barrel architecture can be observed in both normal (**1**) and sensory-deprived (**2**) pups at all observed postnatal ages (P7 and P9). Scale bar 50 μm. **C**, Comparison of barrel size estimated using Vglut 2 staining (barrel size) at P4-6 and P7-9 and spatial extent of functional assemblies (Assembly size) as a function of age. *Two-way ANOVA*, interaction effect:  $F(1,41)=34.74$ ;  $p<0.0001$ . *Post-hoc (Tukey's)*: P4-6 ( $p<0.05$ ) and P7-9, ( $p<0.0001$ ). Data are given as mean  $\pm$  SEM.



# Figure S5. Related to Figure 2

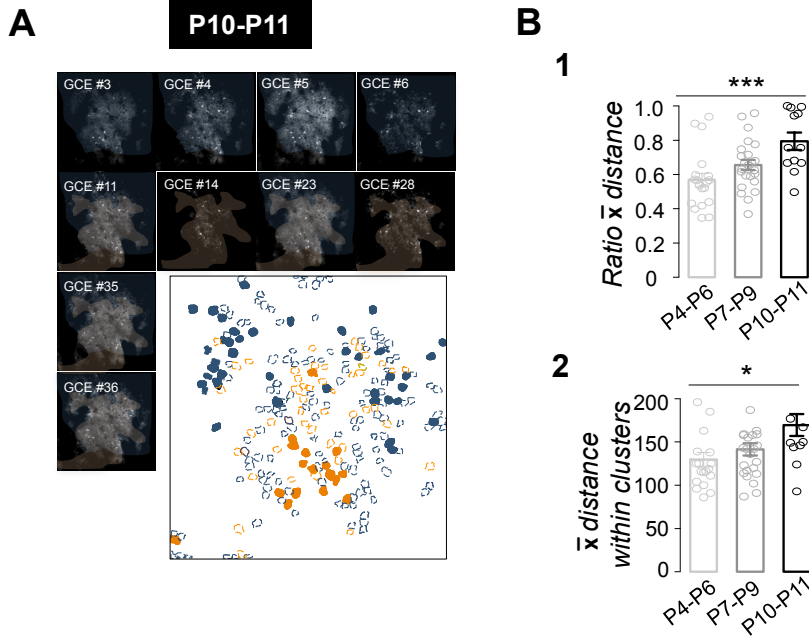


**Figure S5:** (A) Representative time-lapse images showing GCEs occurring in a P11 mouse with the contour map of SOMATA (filled) and RINGS (open), color-coded according to the similarity of their GCE recruitment at P10-11. (B) **1**, Average physical distance between contours recruited in the same GCE clusters divided by the average contour distance. No interaction effect was observed between the different developmental time-point and superficial and deep cortical layers: *Two-way ANOVA* shows no *Interaction* effect ( $F_{(2,49)}=0.36, p=0.69$ ) or *Depth* effect ( $F_{(1,49)}=0.52, p=0.47$ ), but main effect in the *Age* factor ( $F_{(2,49)}=6.76, p=0.002$ ). *Post hoc* (Tukey's) P4-6 vs. P10-11 ( $p<0.001$ ). **2**, Mean physical distance between contours belonging to the same assembly for superficial and deep layers. No interaction effect was observed between the different developmental time-points and cortical depth: *two way ANOVA*,  $F_{(2,49)}=0.12, p=0.88$ ; *Depth* factor,  $F_{(1,49)}=2.47, p=0.12$ . Main effect in the *Age* factor ( $F_{(1,49)}=4.67, p=0.01$ ). *Post hoc* (Tukey's) P4-6 vs. P10-11 ( $p<0.05$ ). Each circle represents a FOV from superficial and deep layers. Data are given by mean  $\pm$  SEM.

# Figure S6. Related to Figure 3

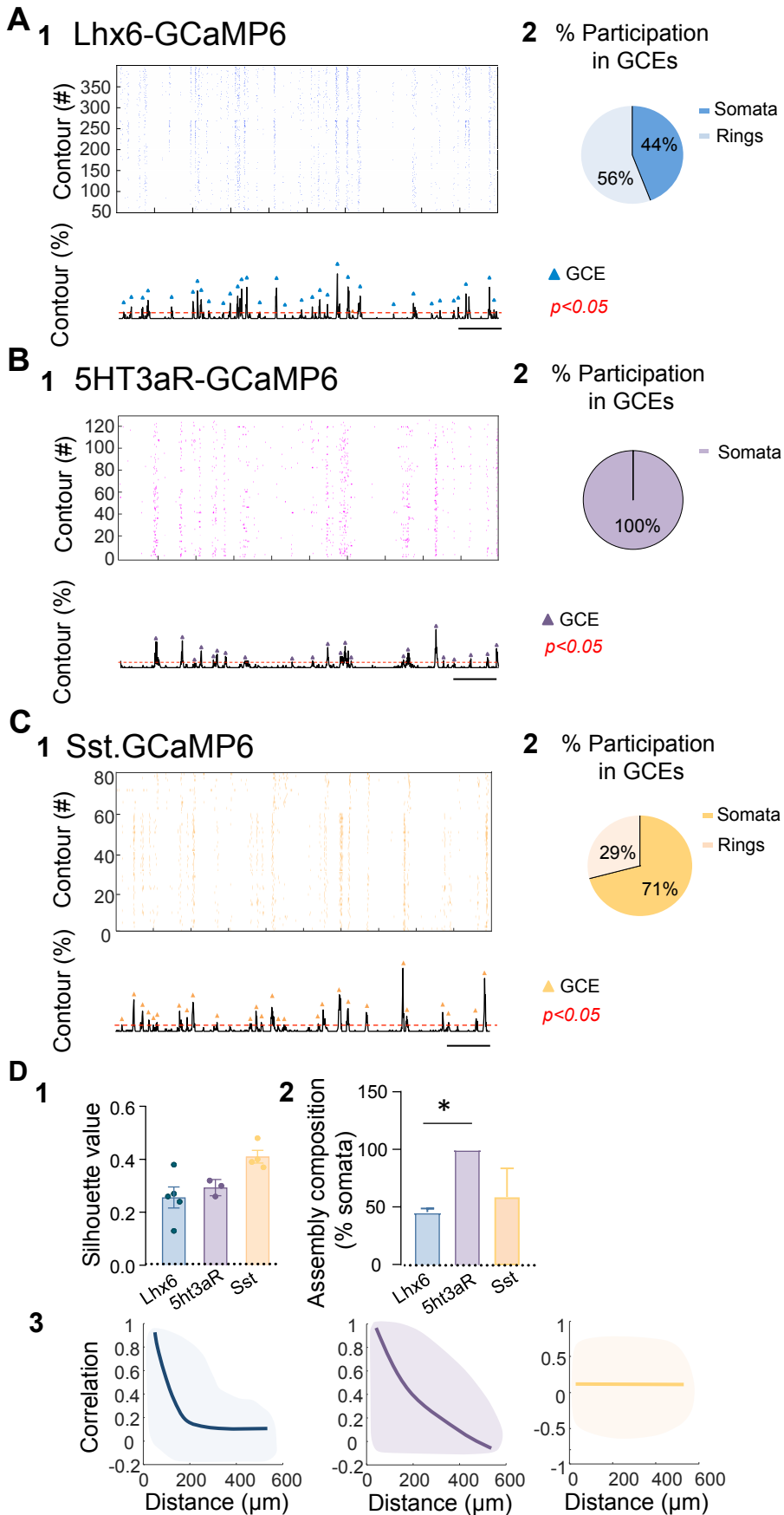


**Figure S6: (A, B and C) 1**, Representative rasterplot indicating detected calcium events in all imaged contours as a function of time from Lhx6-GCaMP6, 5HT3aR-GCaMP6 and Sst-GCaMP6- pups at P8. Note that panel **A** uses the same dataset as illustrated in Fig.2 of Duan et al (companion paper), except that the contours in the rasterplot illustrated here include RINGS and not only SOMATA. Histogram below shows the fraction of active contours as a function of time. Blue triangles indicate GABAergic calcium events (GCE) based on a statistical threshold (dotted red line,  $p < 0.05$ ). Scale bar, 1min. **2**, Percentage of RINGS and SOMATA participation in GCEs. **(B) 1**, Purple triangles indicate GABAergic calcium events (GCE) based on a statistical threshold (dotted red line,  $p < 0.05$ ) in a 5HT3aR.GCaMP6s pup. **2**, Percentage of RINGS and SOMATA participation in GCEs. **(C) 1**, Yellow triangles indicate GABAergic calcium events (GCE) based on a statistical threshold (dotted red line,  $p < 0.05$ ) in a Sst.GCaMP6s.GCaMP6s pup. **2**, Percentage of RINGS and SOMATA participation in GCEs. **(D) 1**, Functional coherence of clustered assemblies (*Silhouette* value) in Lhx6.GCaMP6s (blue), 5HT3aR.GCaMP6s (purple) and Sst.GCaMP6s (Yellow). FOV that presented no assemblies were excluded from the analysis (5-HT3aR,  $n=2$  and Sst,  $n=3$ ). *Two-way ANOVA*:  $F_{(2, 9)}=6.08$ ;  $p=0.02$ . Post-hoc *Tukey's* showed differences when comparing Lhx6 vs. Sst,  $p < 0.05$ . **2**, Percentage of SOMATA contributing to assemblies. *Two-way ANOVA*:  $F_{(2, 10)}=4.54$ ;  $p=0.03$ . Post-hoc *Tukey's* indicate differences between Lhx6.GCaMP6s and 5-HT3aR ( $p < 0.05$ ), showing that perisomatic RINGS contributing to assemblies are mainly MGE derived. Each dot represents a FOV. Values are given by mean  $\pm$  SEM. **3**, Scatter plot visualizing the effect of distance on correlation between pairs of cells in a representative case for Lhx6.GCaMP6s (blue), 5HT3aR.GCaMP6s (purple) and Sst.GCaMP6s (yellow).

**Figure S7. Related to Figure 5**

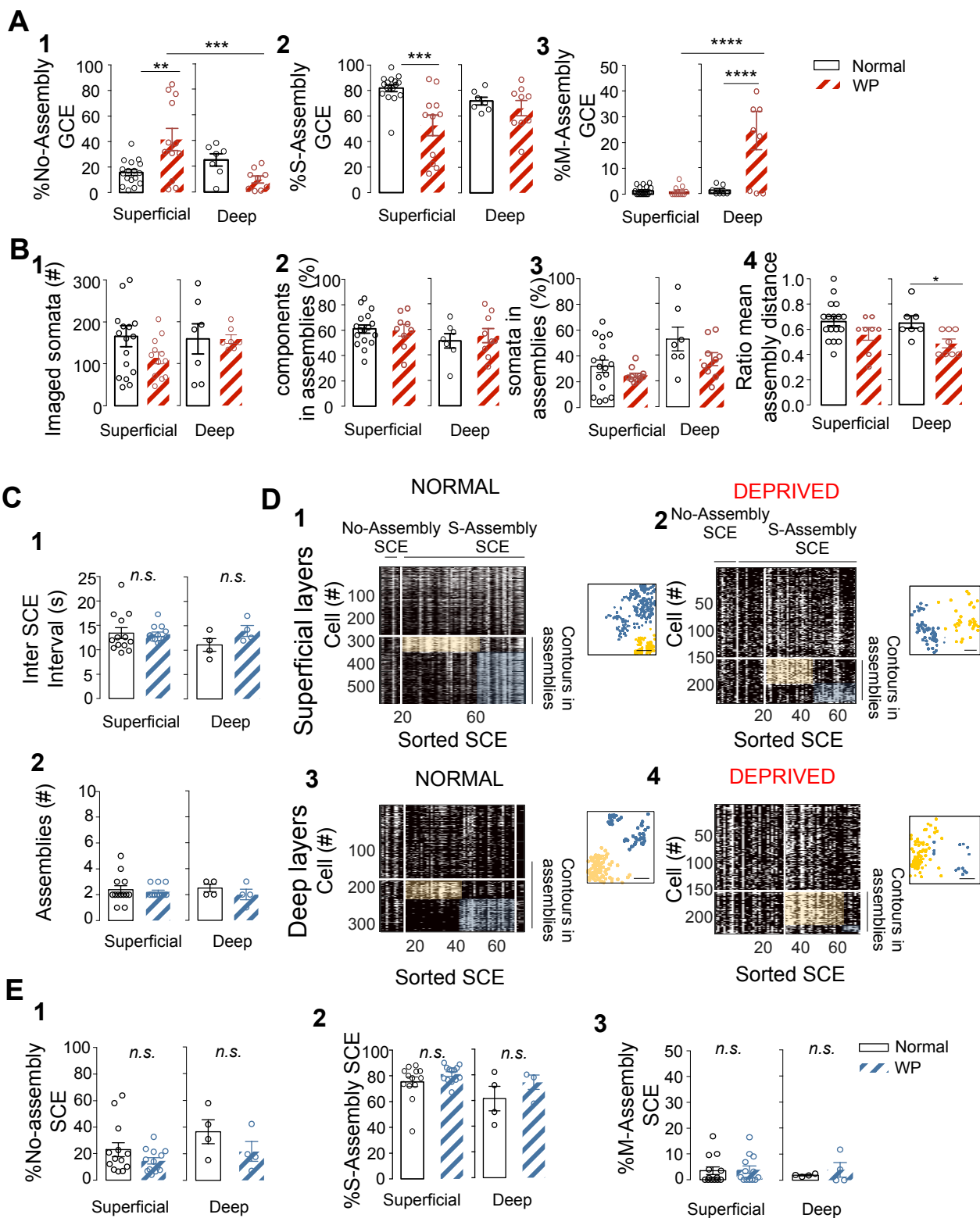


**Figure S7: (A)** Two-way ANOVA (and subsequent *Tukey's post-hoc test*) was performed to analyze the effects of sensory deprivation (deprived (striped red) and normal (black)) in Gad67-GCaMP6 pups at P7-9 in superficial and deep cortical layers. **1**, Percentage of GCEs that did not display any assembly structure. Interaction effect two-way ANOVA  $F_{(1,40)}=15.03$ ,  $p=0.004$ . *Post-hoc* comparisons: WP(superficial) vs. normal (superficial) and WP (deep),  $p<0.01$  and  $p<0.001$ , respectively. **2**, Percentage of GCEs recruiting a single assembly. Interaction effect, two-way ANOVA  $F_{(1,40)}=4.57$ ,  $p=0.038$ . *Post-hoc* comparisons: WP (superficial) vs. normal (superficial),  $p<0.001$ . **3**, Percentage of GCEs recruiting multiple assemblies. Interaction effect, two-way ANOVA  $F_{(1,40)}=13.39$ ,  $p=0.0007$ . *Post-hoc* comparisons: WP (deep) vs. normal (deep) and WP (superficial),  $p<0.0001$ . **(B) 1**, Total number of imaged somata shows no difference between conditions. Two-way ANOVA: no Interaction effect ( $F_{(1,40)}=0.78$ ,  $p=0.38$ ), or WP effect ( $F_{(1,40)}=0.81$ ,  $p=0.35$ ). **2** and **3**, percentage of components **(2)** and cells **(3)** recruited in assemblies. **2**, Two-way ANOVA: no Interaction effect ( $F_{(1,40)}=0.28$ ,  $p=0.59$ ), or WP effect ( $F_{(1,40)}=0.10$ ,  $p=0.74$ ). **3**, Two-way ANOVA: no Interaction effect ( $F_{(1,40)}=0.44$ ,  $p=0.50$ ), or WP effect ( $F_{(1,40)}=2.69$ ,  $p=0.10$ ). **4**, Averaged anatomical distance between contours recruited in the same GCE assembly divided by the average contour distance. Main WP effect was observed in deep layers: two-way ANOVA  $F_{(1,36)}=8.6$ ,  $p=0.005$  and subsequent *post-hoc (Tukey's)* comparisons normal vs. WP,  $p<0.05$ . **(C, D, E)** Two-way or one-way ANOVA (and subsequent *Tukey's post-hoc test*), were performed to analyze differences between WP (striped blue) and normal (black) WT pups injected with AAV1.hSyn.GCaMP6s.GFP at P0. Each circle represents one FOV (WP superficial: 13 FOVs and 3 mice; WP deep: 4 FOVs, 3 mice; normal superficial: 13 FOVs, 6 mice, normal deep: 4 FOVs, 3 mice). No differences were observed when comparing normal vs. deprived conditions or superficial vs. deep cortical layers neither in each of the factors in: **(C) 1**, Inter SCE interval: Two-way ANOVA  $F_{(1,30)}=0.44$ ,  $p=0.51$  and no main deprivation effect:  $F_{(1,30)}=1.25$ ,  $p=0.27$ ; **2**, the number of functional assemblies, two-way ANOVA  $F_{(1,30)}=0.26$ ,  $p=0.607$ , no main deprivation effect:  $F_{(1,30)}=0.96$ ,  $p=0.334$  and **(E) 1**, the percentage of SCEs without assembly structure: two-way ANOVA  $F_{(1,30)}=0.25$ ,  $p=0.618$ , no main deprivation effect:  $F_{(1,30)}=3.23$ ,  $p=0.08$ , **2**, the percentage of SCEs recruiting single assemblies two-way ANOVA Interaction effect ( $F_{(1,30)}=0.42$ ,  $p=0.519$ ) and WP effect ( $F_{(1,30)}=3.33$ ,  $p=0.07$ ) and **3**, the percentage of SCEs recruiting multiple assemblies, two-way ANOVA Interaction effect ( $F_{(1,30)}=0.16$ ,  $p=0.68$ ), no main Deprivation effect ( $F_{(1,30)}=0.36$ ,  $p=0.55$ ). **(D) 1**, Rasterplots of SCEs sorted following clustering in one representative imaging session at P9 in superficial layers of normal and sensory deprived pups. Contour maps are color-coded according to assembly membership. Each circle represents a FOV. Data are given as Mean  $\pm$  SEM